Human Precision-Cut Tumour Slices and Immune Co-Culture Systems to Assess and Enhance Immunotherapy Response in Cholangiocarcinoma

Maria-Danae Jessel [1], Owen McGreevy [1], Timothy M Gilbert [1,2], Marie Held [3], Thomas Waring [3], Lekh N Dahal [1], Hassan Z Malik [2], Christopher E Goldring [1], Laura E Randle [1]

[1] Department of Pharmacology and Therapeutics, University of Liverpool, Liverpool, UK [2] Hepatobiliary Surgery, Liverpool University Hospitals NHS Foundation Trust, Liverpool, UK [3] Centre for Cell Imaging, University of Liverpool, Liverpool, UK

① Introduction

- CCA is an aggressive biliary tract malignancy [1] with a 5-10% 5-year survival rate [2].
- UK incidence has doubled since 2002 [2], with diagnoses approaching hepatocellular carcinoma in 2022 [3].
- Response to immune checkpoint inhibitors (ICIs) remains poor [4,5,6].
- Enrichment of immunosuppressive myeloid cells and excluded/exhausted cytotoxic T cells in the CCA tumour microenvironment (TME) contributes to ICI resistance [7,8,9].
- Dual targeting of TAMs and MDSCs enhanced anti-PD-1 therapy in murine CCA models [10].
- Improved human-relevant preclinical models are needed to tailor therapeutic approaches [11,12].

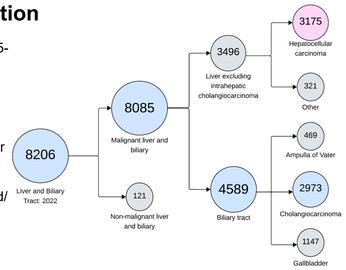

Figure 1. Tree diagram on UK liver and biliary tract diagnoses in 2022. Taken from [9].

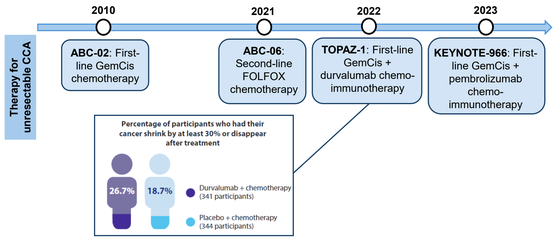

Figure 2. Timeline of phase III clinical trials in chemo-immunotherapy for advanced CCA. Image taken from [4].

Aim: To develop and apply complementary human *in vitro* and *ex vivo* models to investigate immunosuppression and identify strategies to enhance immunotherapy responses in CCA.

② Methodology

1) Human precision-cut tumour slices (hPCTS)

- hPCTS generated and cultured based on the Kenerson *et al.*[13] STAR protocol.
- 5mm diameter, 250µm thick hPCTS were generated using the Krumdieck Tissue Slicer.
- hPCTS were cultured on Millicell® organotypic inserts for up to 15 days.
- Staurosporine was tested for 48-hour dose response capability of hPCTS using MTS assay (490nm) and immunohistochemistry (IHC) staining for cleaved-caspase 3 (CC3).
- ICB response assessed by RT-qPCR (IL-1β, TNF-α, TGF-β, MCP-1, IL-10, IL-6) relative to matched IgG controls.
- PBMC migration into hPCTS was evaluated via co-culture with CFSE-labelled autologous PBMCs for 6 days; hPCTS were then fixed, DAPI-stained, and imaged by confocal microscopy.
- Statistics: GraphPad Prism (v10.5.0); * p ≤ 0.05, ** p ≤ 0.01, *** p ≤ 0.001, **** p. ≤ 0.0001.

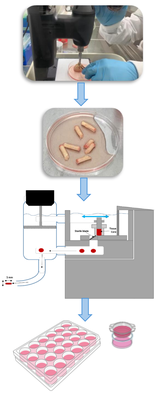

Figure 3. CCA sample processing and hPCTS generation.

2) *In vitro* tumour-associated macrophage (TAM) / myeloid-derived suppressor cell (MDSC)-CD8⁺ T cell co-culture model

- Protocol adapted from Benner *et al.*[14] and Choi *et al.*[15].
- CCA tumour-conditioned medium (TCM) generated from intrahepatic CCA (iCCA) hPCTS or iCCA HuCC-T1 cell line.
- PBMCs differentiated into TAMs / MDSCs using TCM and cytokine cocktail.
- Flow cytometry using BD FACS Canto II was used to evaluate TAM (CD163-PE, CD206-AF488) and MDSC (CD14-PerCP-Cy5.5, CD15-AF488) phenotype.
- CD8⁺ T cells will be isolated from autologous PBMCs and labelled with CFSE.
- TAMs / MDSCs and CD8+ T cells will be co-cultured (0-72 hours).

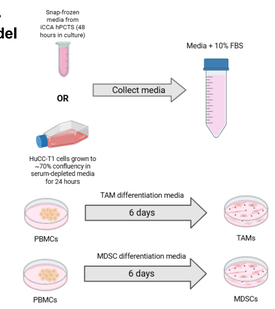

Figure 4. iCCA TCM generation and TAM / MDSC differentiation timeline. Made using BioRender.com.

③ Results

1) CCA hPCTS respond to 48-hour staurosporine treatment in a dose-dependant manner.

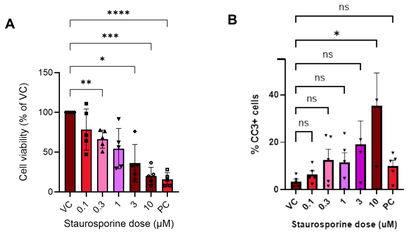

Figure 5. (A) Cell viability of CCA hPCTS after 48-hour treatment with staurosporine. MTS assay results shown relative to vehicle control (VC); mean ± SEM, n=5. VC = 0.5% DMSO; Positive control (PC) = 50% DMSO. (B) Percentage of CC3+ cells of CCA hPCTS after 48-hour treatment with staurosporine. Statistical test: RM One-way ANOVA with Dunnett's multiple comparisons vs VC.

- CCA hPCTS respond to treatment with staurosporine in a dose-dependent manner, with cell viability decreasing and percentage of CC3 increasing with increasing concentration of drug.
- This supports the suitability of hPCTS as a viable, pharmacologically responsive, and dynamic *ex vivo* model for pharmacological treatment studies.

2) Preliminary 72-hour treatment of CCA hPCTS with ICIs induced dose-dependent, gene-specific transcriptional changes.

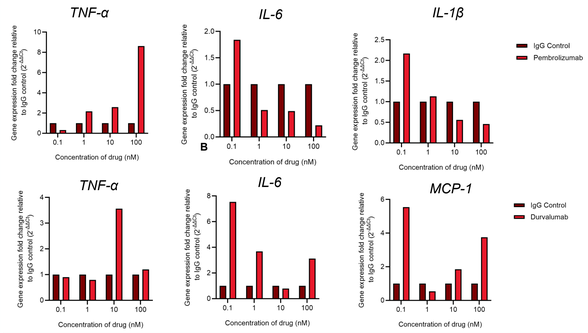

Figure 6. ICI-induced gene expression changes in CCA hPCTS treated for 72 hours. Top: pembrolizumab; bottom: durvalumab. Fold change in gene expression measured by RT-qPCR relative to matched IgG controls ($2^{-\Delta\Delta Ct}$; n=1).

Preliminary treatment with anti-PD-1 and anti-PD-L1 inhibitors induced clear dose-dependent and gene-specific changes, supporting immunological responsiveness of CCA hPCTS *ex vivo*.

3) Autologous PBMCs can infiltrate and persist in CCA hPCTS in prolonged *ex vivo* culture.

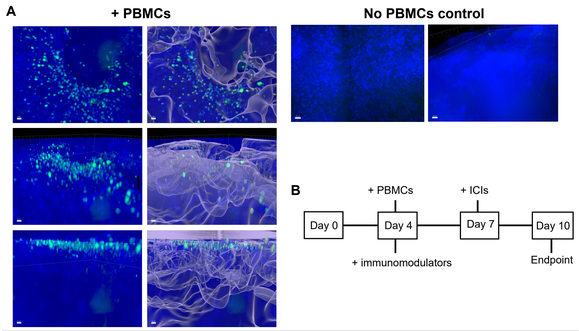

Figure 7. (A) CFSE-labelled autologous PBMCs (1 × 10⁶/slice) were added to hPCTS on Days 2 and 4. After 6 days of co-culture, slices were DAPI-stained, fixed, and imaged by confocal microscopy (2 µm Z-stacks). Representative raw images and segmented reconstructions are shown (CFSE, green; DAPI, blue). Scale bar = 20 µm. (B) Proposed experimental timeline: Day 0, culture start; Day 4, PBMC + immunomodulators; Day 7, ICIs; Day 10, endpoint.

CFSE⁺ autologous PBMCs can infiltrate and persist in hPCTS for at least 6 days *ex vivo*, with no signal observed in negative controls, enabling immune-augmented hPCTS cultures for immunomodulator testing.

4) Autologous PBMC infiltration and migration can be quantitively measured in CCA hPCTS.

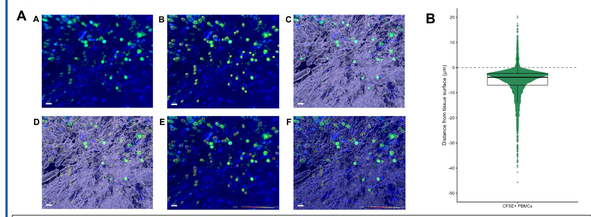

Figure 8. Quantification of PBMC infiltration in hPCTS. (A) Representative confocal image from a PBMC–hPCTS co-culture showing sequential image analysis steps: (A) raw image (CFSE-labelled PBMCs, green; DAPI tissue, blue); (B) CFSE⁺ cell spot detection; (C) tissue surface segmentation; (D) spot-to-surface overlay; (E) CFSE⁺ cells colour-coded by distance from tissue surface; (F) final combined output for infiltration quantification. Scale bars = 50 µm. B) Violin plot showing the distribution of distances of CFSE⁺ PBMCs from hPCTS surface. Negative values indicate cells within the tissue. Overlayed box plot shows median and interquartile range. Median infiltration distance = -3.86 µm.

- Infiltration distance and distribution quantified using Fiji and Imaris software.
- 3D reconstruction preserves spatial context of immune migration.
- Developed a quantitative framework that enables assessment of immune cell infiltration in preserved 3D human tumour architecture.
- Platform applicable for evaluating treatment-induced changes.

5) hPCTS-derived TCM drives stronger CD163⁺/CD206⁺ TAM polarisation than HuCC-T1 cell line TCM after 6-day *in vitro* differentiation.

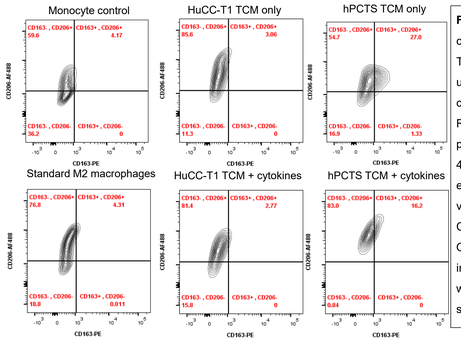

Figure 9. Flow cytometric analysis of TAMs differentiated under different conditions. Representative contour plots show CD206-AF 488 vs CD163-PE expression within viable, single-cell, CD11b⁺ population. Quadrant gates indicate co-expression, with percentages shown in red.

- TCM source affected TAM phenotype (n = 3).
- hPCTS-derived TCM generated higher CD163⁺/CD206⁺ TAM-like populations than HuCC-T1 TCM.
- Patient-derived TCM may better model CCA-associated macrophage polarisation.

6) hPCTS-derived TCM drives a distinct CD14⁺/CD15⁺ MDSC-like phenotype after 6-day *in vitro* differentiation.

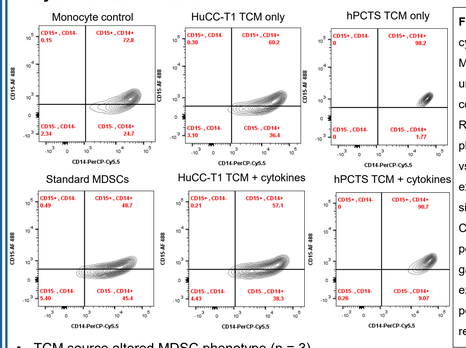

Figure 10. Flow cytometric analysis of MDSCs differentiated under different conditions. Representative contour plots show CD15-AF 488 vs CD14–PerCP-Cy5.5 expression within viable, single-cell, CD11b⁺, CD33⁺, HLA-DR$^{low/-}$ population. Quadrant gates indicate co-expression, with percentages shown in red.

- TCM source altered MDSC phenotype (n = 3).
- hPCTS-derived TCM enriched CD14⁺/CD15⁺ MDSC-like cells, indicating distinct myeloid polarisation.
- HuCC-T1 TCM generates a more heterogeneous phenotype, resembling media controls.
- Patient-derived TCM may provide improved modelling of CCA-associated myeloid differentiation.

④ Conclusions

- CCA hPCTS exhibited dose-dependent cytotoxic responses to staurosporine, supporting their suitability as a viable *ex vivo* platform for pharmacological testing.
- Preliminary 72-hour durvalumab and pembrolizumab treatments induced dose-dependent transcriptional changes relative to matched IgG controls, including altered TNF-α, IL-6, IL-1β and MCP-1 expression, suggesting modulation of inflammatory and immune signalling pathways.
- Autologous PBMCs efficiently infiltrated CCA hPCTS, demonstrating preserved chemotactic responsiveness and supporting the use of exogenous immune cells to enhance physiological relevance for immunomodulator testing, as well as adoptive cell therapy studies (e.g. CAR-T cells).
- hPCTS-derived TCM promoted a stronger TAM phenotype (CD163⁺/CD206⁺) and a distinct CD14⁺/CD15⁺ MDSC-like phenotype compared with HuCC-T1-derived TCM, suggesting that patient-derived models may better recapitulate the complex CCA tumour microenvironment.
- Overall, these complementary *in vitro* and *ex vivo* human platforms provide a translational framework for investigating tumour–immune interactions and identifying strategies to enhance immunotherapy responses in CCA.

⑤ Future Work

- Flow cytometric functional assessment of T cell responses to validate the immunosuppressive capacity of CCA-conditioned TAMs/MDSCs.
- Evaluate candidate immunomodulators in TAM/MDSC–CD8⁺ T cell co-cultures and assess effects on T cell activation, proliferation, and function.
- Translate promising *in vitro* findings to CCA hPCTS to determine whether targeting suppressive myeloid cells enhances anti-tumour immune responses.
- Use the CFSE-labelled PBMC migration assay to assess treatment-induced changes in immune cell infiltration and distribution within CCA hPCTS.
- Test immune checkpoint inhibitors and combination therapies in augmented CCA hPCTS containing exogenous immune cells to explore improved treatment responses.

E: mdjessel@liverpool.ac.uk

Randle Lab Website

Acknowledgements

We thank the University of Liverpool Human Liver Research Facility, Centre for Cell Imaging, and Histology SRF for their support and technical assistance in this work. We also thank the patients and their families for generously donating the samples that made this work possible.

References

[1]Banales JM, et al. Cholangiocarcinoma 2020: the next horizon in mechanisms and management. Nat Rev Gastroenterol Hepatol. 2020 Sep;17(9):557-588. doi: 10.1038/s41575-020-0310-z. Epub 2020 Jun 30. PMID: 32606456; PMCID: PMC7447603.
[2]Tataru D, et al. Cholangiocarcinoma across England: Temporal changes in incidence, survival and routes to diagnosis by region and level of socioeconomic deprivation. JHEP Rep. 2023 Dec 15;6(3):100983. doi: 10.1016/j.jhepr.2023.100983. PMID: 38357420; PMCID: PMC10865079.
[3]NCRAS Get Data Out Programme, "Liver and biliary tract", https://www.cancerdata.nhs.uk/getdataout/liver
[4]Do-Youn Oh, et al. Plain Language Summary of the TOPAZ-1 Study: Durvalumab and Chemotherapy for Advanced Biliary Tract Cancer, Future Oncology, 19:34, 2277-2289, September 2023. DOI: 10.2217/fon-2023-0468
[5]Oh DY, et al. Durvalumab plus Gemcitabine and Cisplatin in Advanced Biliary Tract Cancer. NEJM Evid. 2022 Aug;1(8):EVIDoa2200015. doi: 10.1056/EVIDoa2200015. Epub 2022 Jun 1. PMID: 38319896.
[6]Kelley RK, Ueno M, Yoo C, Finn RS, Furuse J, Ren Z, et al. Pembrolizumab in combination with gemcitabine and cisplatin compared with gemcitabine and cisplatin alone for patients with advanced biliary tract cancer (KEYNOTE-966): a randomised, double-blind, placebo-controlled, phase 3 trial. The Lancet. 2023;401(10391):1853-65.
[7]Job S, et al. Identification of Four Immune Subtypes Characterized by Distinct Composition and Functions of Tumor Microenvironment in Intrahepatic Cholangiocarcinoma. Hepatology 72(3):p 965-981, September 2020. | DOI: 10.1002/hep.31092
[8]Loeuillard E, et al. Immunobiology of cholangiocarcinoma. JHEP Reports. 2019;1(4):297-311.
[9]Jessel M-D, et al. Targeting the tumor microenvironment in cholangiocarcinoma to improve immune checkpoint blockade: potential strategies and translational pre-clinical models. Clinical & Translational Immunology. 2025;14(10):e70057
[10]Loeuillard E, et al. Targeting tumor-associated macrophages and granulocytic myeloid-derived suppressor cells augments PD-1 blockade in cholangiocarcinoma. The Journal of Clinical Investigation. 2020;130(10):5380-96.
[11]Banales JM, et al. Cholangiocarcinoma 2026: status quo, unmet needs and priorities. Nature Reviews Gastroenterology & Hepatology. 2026;23(1):65-96.
[12]Calvisi DF, et al. Criteria for preclinical models of cholangiocarcinoma: scientific and medical relevance. Nature Reviews Gastroenterology & Hepatology. 2023;20(7):462-80.
[13]Kenerson HL, *et al*. Protocol for tissue slice cultures from human solid tumors to study therapeutic response. STAR Protocols 2021; 2: 100574.
[14]Benner B, et al. Generation of monocyte-derived tumor-associated macrophages using tumor-conditioned media provides a novel method to study tumor-associated macrophages in vitro. J. Immunotherapy Cancer 7, 140 (2019). https://doi.org/10.1186/s40425-019-0622-0
[15]Choi JE, et al. Isolation of human and mouse myeloid-derived suppressor cells for metabolic analysis. STAR Protocols. 2022; 3(2):101389. DOI: 10.1016/j.xpro.2022.101389.